# Inversion Asymmetry in Heterostructures of Zinc-Blende Semiconductors: Interface and External Potential versus Bulk Effects

O. Krebs,[1] D. Rondi,[2] J. L. Gentner,[3] L. Goldstein,[3] and P. Voisin[1]
[1]*Laboratoire de Physique de la Matière Condensée de l'Ecole Normale Supérieure, 24 rue Lhomond, F75005 Paris, France*
[2]*Laboratoire Central de Recherche, Thomson-CSF, F91400 Orsay, France*
[3]*Alcatel-Alsthom Research, Route de Nozay, F91460 Marcoussis, France*
(Received 27 October 1997)

The direct observation of electric-field-induced optical anisotropy in InGaAs-InP quantum wells is reported. The analysis of this effect shows that hitherto neglected heavy- and light-hole couplings at the minizone center due to interface and external potential inversion asymmetries play a much stronger role than the classical bulk inversion asymmetry. The giant electropleochroism previously reported by Kwok *et al.* is quantitatively explained. [S0031-9007(98)06420-5]

PACS numbers: 73.20.Dx, 78.20.Fm, 78.20.Jq, 78.66.–w

Inversion asymmetry in heterostructures of zinc-blende semiconductors governs a variety of properties such as the parity degeneracy of band dispersions, spin-orientation phenomena, or second order optical nonlinearities in quantum well (QW) structures. Yet, the origin of the leading terms is a matter of current discussion. Asymmetry may originate from the bulk materials, the external potential, or the heterointerfaces themselves. The first two contributions have been extensively discussed in the frame of the $\mathbf{k} \cdot \mathbf{p}$ theory [1,2]. However, the role of interfaces, although identified a long time ago in the context of tight-binding calculations [3], has been overlooked until recently. Several experimental observations [4–6] have renewed the interest in this matter. In particular, the classical envelope function theory (EFT) has failed to explain the difference between systems where the well and barrier material share a common atom, or CA-QWs, and those where they do not, or *no-common-atom* (NCA) QWs. The latter generally [5,6] show a large anisotropy of the optical absorption with respect to the in-plane polarization of the optical wave, while the former do not. Moreover, it was observed in biased CA-QWs that the parity forbidden transitions are strongly polarized, while the parity allowed transitions remain unpolarized [7]. The EFT predicts no polarization dependence at all in any of these circumstances, and must be modified to account for these observations. There are two controversial aspects: (i) What is the main source of inversion asymmetry in semiconductor QWs? (ii) Is the leading term a coupling of heavy- and light-holes at the minizone center ($\mathbf{k}_t = \mathbf{0}$) or a $\mathbf{k}_t$-dependent coupling originating from the interactions with remote bands? In order to clarify these questions, we report in this Letter the direct measurements of the electric-field-induced optical anisotropy or quantum confined Pockels effect (QCPE) in (InGa)As-InP NCA-QWs. The interpretation of the experimental data within the $H_{\mathrm{BF}}$ model [8] is satisfactory, and proves that the hitherto neglected coupling of the hole spin components at $\mathbf{k}_t = \mathbf{0}$ by the interface and potential asymmetries plays the dominant role. This theory also explains the previous observation of a QCPE in biased GaAs-AlAs CA-QWs [7].

In the classical EFT, each host is described by a simplified quasi-Ge $\mathbf{k} \cdot \mathbf{p}$ Hamiltonian, and the interfaces are treated as a scalar potential. The $J_z = \pm 3/2$ heavy-holes and the $J_z = \pm 1/2$ light-particle states are not coupled at $\mathbf{k}_t = (\mathbf{k}_x, \mathbf{k}_y) = \mathbf{0}$. This remains true when the full $8 \times 8$ Pikus and Bir Hamiltonian [9] is used together with the usual boundary conditions, as was done recently by Zhu and Chang [1]. However, this result is in contradiction with the fact that a slab of III-V semiconductor grown along the $[0, 0, 1]$ direction and submitted to a potential $V(z)$ having no inversion symmetry (such as an interface band offset or an electrostatic potential) has the $C_{2v}$ point group symmetry. Indeed, in this case, the $|3/2, \pm 3/2\rangle$ and $|3/2, \pm 1/2\rangle$ heavy-hole ($H$) and light-hole ($L$) states cannot be pure eigenstates. This is because not only the inversion symmetry of the diamond lattice but also the fourfold rotoinversion symmetry of the zinc-blende crystal is broken by $V(z)$. In the perturbative limit of a tight-binding approach [5], the $H$ and $L$ states are coupled at $\mathbf{k}_t = \mathbf{0}$ by a first order term proportional to the potential asymmetry. This point of view is supported by the recent generalized boundary condition (GBC) theory [10] in which the hole envelope function boundary conditions are generalized and mix the $H$ and $L$ spin components. In the heuristic $H_{\mathrm{BF}}$ *model* [8], the same symmetry considerations are treated as a perturbation to the classical EFT. Although the GBC and $H_{\mathrm{BF}}$ theories do not take explicitly into account the native asymmetry of bulk III-Vs, they both explain fairly well the giant optical anisotropy of NCA-QWs, and agree with tight-binding calculations [5]. On the contrary, the bulk and field-induced anisotropy terms considered by Zhu and Chang [1] could not account quantitatively for the anisotropy observed in the luminescence of biased GaAs-AlAs QWs [7], and would not explain the observations in NCA-QWs [5].

The discussion will be focused on a sample S1 which consists of a state-of-the-art quality, metal-organic chemical-vapor deposition (MOCVD) grown 50-period

 0031-9007/98/80(26)/5770(4)$15.00 

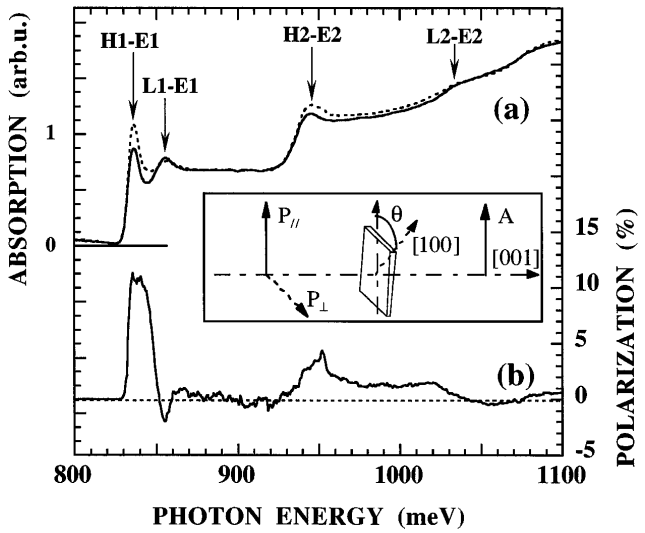


FIG. 1. Optical absorption spectra of sample S1 recorded at 77 K, under zero bias, with light linearly polarized along the $[1,1,0]$ and $[-1,1,0]$ directions (*a*). Relative difference of these spectra or polarization spectrum (*b*). The inset shows a scheme of the experimental setup.

InGaAs(113 Å)-InP (100 Å) MQW forming the intrinsic part of a *p-i-n* diode. The built-in electric field $F_0$ is 7 kV/cm [11]. X-ray diffraction shows that the sample is strain-free. Optical transmission spectra are recorded at 77 K, under normal incidence. The light source is a halogen lamp filtered by a grating spectrometer. The sample is placed between two Glan-prism polarizers, and can be rotated around the $[0,0,1]$ growth axis, as illustrated in the inset of Fig. 1. The absorption spectra obtained from the transmission data with light linearly polarized along the $[1,1,0]$ and $[-1,1,0]$ directions and the relative difference of these spectra, or polarization spectrum, are shown in Figs. 1(*a*) and 1(*b*). These results witness to the excellent quality of the sample and illustrate the existence of a huge dichroism (up to 11%) in the spectral region between the $H1$-$E1$ and $L1$-$E1$ transitions. A replica of this effect is also observed between the $H2$-$E2$ and $L2$-$E2$ transitions. As previously discussed [5,8], this in-plane optical anisotropy is due to the specific interface bonds (here, P-(InGa) and As-In) existing in NCA QWs.

The field-dependent absorption and polarization spectra are displayed in Figs. 2 and 3, together with the result of our calculations. The quantum confined Stark effect (QCSE) data shown in Fig. 2 illustrate the well-known redshift of the first transitions, associated with the emergence of new transitions which were parity forbidden at $F = 0$. The width of the transitions does not increase significantly, which proves that the electric field is quite homogeneous through the MQW region [11]. As seen on Fig. 3(*a*), the optical anisotropy is strongly affected by the electric field. The polarization spectrum basically consists of two regions, the first one between the $H1$-$E1$ and $H2$-$E1$ transitions and the second one between the $H2$-$E1$ and $L1$-$E1$ transitions. The polarization rates of these transitions undergo different changes, which produce both qualitative and quantitative changes in the polarization spectrum. The inset shows that the field dependence of the polarization at $h\nu = 838$ meV ($H1$-$E1$ transition) is linear at low field.

The optical anisotropy of NCA-QWs is understood, within the GBC [10] or $H_{BF}$ [8] theories, in terms of two potentials ($\delta V_1 = V_1'$-$V_2$ and $\delta V_2 = V_2'$-$V_2$ in the notations of Ref. [8]) localized at the two interfaces and mixing the $H$ and $L$ states at the minizone center. When an axial electric field $F$ is turned on, the situation is changed in three different ways: (i) The different subbands of each particle $(H, L, E)$ are mixed by the electrostatic potential $eFz$; (2) the related breakdown of the parity selection rules introduces new transitions in the optical spectrum; (3) the bulk properties are affected by the symmetry reduction due to the asymmetric perturbation. The corresponding changes of the optical spectra are easily understood in the perturbative framework of the $H_{BF}$ model, where the actual Hamiltonian $H_{BF} = H_{BF}^0 + H^F$ is expanded in the truncated basis formed by the $F = 0$ bound eigenstates of the usual square-well EFT Hamiltonian. In this basis, the $H_{BF}$ matrix elements are written in a simple analytical form. $H_{BF}^0$ contains diagonal corrections to the energy levels, proportional to the squared envelope function amplitudes at the interfaces, and off-diagonal terms mixing the heavy- and light-hole states, proportional to the product of the $H$ and $L$ envelope amplitudes at the interfaces. $H^F$ contains two different

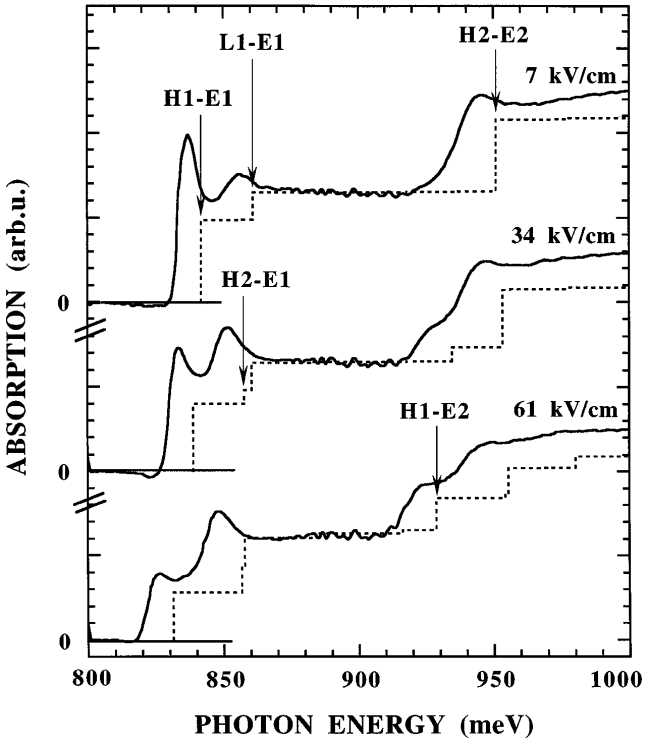


FIG. 2. Optical absorption spectra for various values of the electric field, and the corresponding theoretical spectra. The calculation takes into account the diagonal corrections of the $H_{BF}$ model.

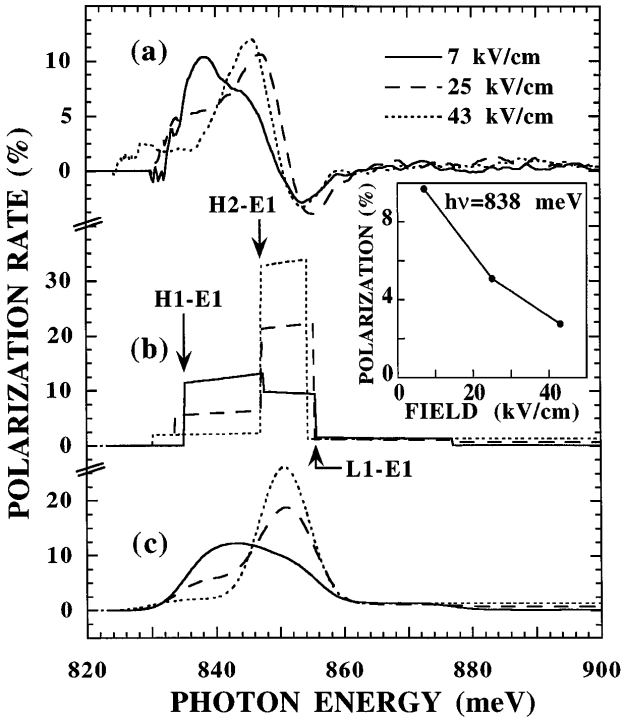


FIG. 3. Polarization spectra for various values of the electric field (*a*), corresponding calculations (*b*), and the same calculations, including a 6 meV phenomenological broadening of the transitions (*c*). The inset shows the field dependence of the polarization rate for $h\nu = 838$ meV.

contributions: (i) The classical $eFz$ term which mixes, for each particle, the subbands of different indexes. It gives rise to the QCSE, and contributes to the QCPE by changing the respective weights of the left and right interfaces. (ii) There is a *bulk* term proportional to $F$ and to the overlap of the $H$ and $L$ envelope functions, mixing the $H$ and $L$ subbands just like the interface potentials do. The latter term is absent from previous $\mathbf{k}\cdot\mathbf{p}$ theories of the Pockels effect [12,13] and has no equivalent in the Pikus and Bir Hamiltonian. It is argued in Ref. [14] that the origin for the missing term is the potential $eFz$ being incompatible with the cyclic boundary conditions used in the $\mathbf{k}\cdot\mathbf{p}$ theory. In the $H_{\mathrm{BF}}$ model, this new term appears naturally, as all (slowly or rapidly varying) contributions to the breakdown of the rotoinversion symmetry are treated on the same footing. Again, in this simple-minded approach, the interactions with remote bands considered in Ref. [1] are neglected. When calculating the optical absorption spectrum, the in-plane motion can be treated either in the diagonal approximation, as in Ref. [8] or by expanding the Luttinger Hamiltonian in the same bound eigenstate basis, following the method developed by Bastard *et al.* [15]. We have found only insignificant differences between the optical spectra calculated using either model, although the corresponding valence subband dispersions are spectacularly different. We stress here the drastic difference between the $\mathbf{k}_t = \mathbf{0}$ coupling and the mixing at finite $\mathbf{k}_t$ due to the Luttinger Hamiltonian. The former has little influence on subband dispersions but produces the dramatic optical anisotropy effects, while the latter governs the subband dispersions but actually has little consequence on the optical spectra.

We first examine the fit of the QCSE data displayed in Fig. 2. Taking into account exciton binding energies of the order of 6 meV, the agreement between experiment and theory is very good for all values of the field [11]. In particular, the experimental $H1$-$L1$ splitting (19 meV at $F = 0$) is significantly smaller than the value (23 meV) initially obtained in the EFT approximation. This is because the diagonal correction is much larger for $L1$ than for $H1$ (see numerical values in Table I). The sign of this correction indicates that the dominant interface potential is attractive, which is fully confirmed by the fit of the field-dependent polarization spectra. As the field is increased, the $H1$-$E1$ and $L1$-$E1$ transitions are redshifted, and the parity forbidden $H2$-$E1$ transition gains more oscillator strength. We now concentrate on the QCPE illustrated in Fig. 3. The theoretical curves [Figs. 3(*b*) and 3(*c*)] have been shifted by 6 meV to allow a better comparison with the experimental data. This amounts to assuming that the excitonic features are polarized the same way as the corresponding band-to-band transitions, and to consider equivalent binding energies for the excitons associated with any pair of subbands [16]. Interface potentials $\delta V_1 = -1000$ meV and $\delta V_2 = +50$ meV yield the best fit. The corresponding values of the main $H_{\mathrm{BF}}$ matrix elements are listed in Table I. Figure 3 shows that the general trends of the experimental results are well reproduced, and the agreement becomes rather good if a broadening of the transitions is introduced in the calculation [Fig. 3(*c*)]. These parameters also give a satisfactory description of the QCPE replica observed between $H2$-$E2$ and $L2$-$E2$.

Actual interface compositions depend on the growth conditions, for instance, via the anion exchange mechanism during growth interruption. We have indeed performed the same experiments on an equivalent sample $S2$ grown by Gas-Source molecular-beam epitaxy instead of MOCVD. Significant differences in the shape of the QCPE spectra are observed, leading to different interface potentials $\delta V_1 = -600$ meV, $\delta V_2 = -50$ meV. Altogether, these results clearly indicate that the interfaces, which are responsible for the $F = 0$ optical anisotropy [5,6], are the leading cause of Pockels effect in NCA-QWs.

In the case of common anion (CA) QWs, the $H_{\mathrm{BF}}$ interface potentials are merely the usual valence band

TABLE I. Numerical values (in meV) of the main $H_{\mathrm{BF}}$ matrix elements corresponding to the fit of the QCPE in sample S1.

| $F$ (kV/cm) | $H1$-$H1$ | $L1$-$L1$ | $H1$-$H2$ | $L1$-$L2$ | $H1$-$L1$ | $H2$-$L1$ |
|---|---|---|---|---|---|---|
| 0 | −0.64 | −3.3 | +0.69 | +3.3 | $i$0.84 | $i$1.82 |
| 50 | −0.64 | −3.3 | −10.53 | −10.1 | $i$1.26 | $i$1.82 |

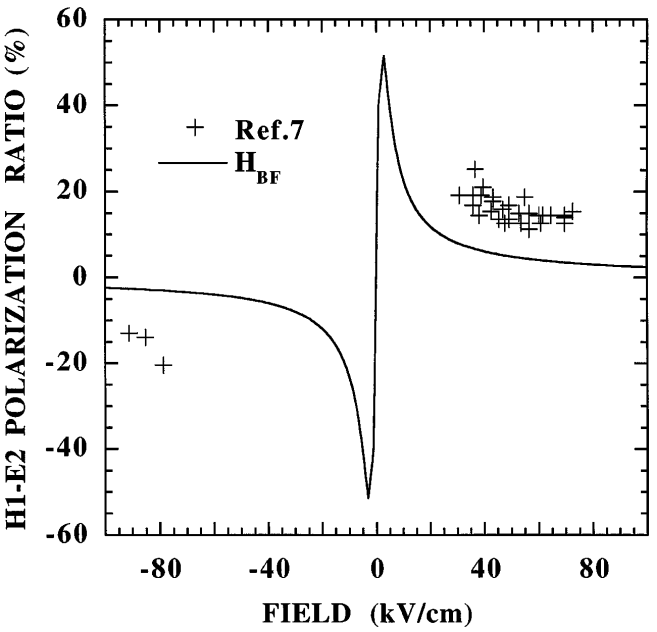


FIG. 4. Polarization rate of the $H1$-$E2$ low temperature luminescence versus applied electric field measured in a 100 Å GaAs-AlAs quantum well (crosses, from Ref. [7]) and corresponding $H_{\mathrm{BF}}$ calculation (solid line).

offset and, if the well is symmetric, they only mix heavy- and light-hole bands of different parities, as required by the corresponding $D_{2d}$ symmetry. Hence, for CA-QWs, the theory contains no adjustable parameter. This is why we finally reexamine the *electropleochroism* effect reported in Ref. [7] and discussed theoretically in Ref. [1]. Kwok *et al.* [7] have investigated carefully the polarization of the low temperature luminescence of a biased GaAs-AlAs MQW. They found that the main $H1$-$E1$ exciton luminescence is completely unpolarized, which is in agreement with our parameter-free calculation and illustrates the importance of the bulk contribution to $H^F$. Indeed we calculate a polarization rate below 1% for the $H1$-$E1$ transition at $F = 100$ kV/cm, while the sole contribution of interfaces would give 5.5%. This means that in CA-QWs the bulk and interface contributions to the Pockels effect tend to cancel each other for allowed transitions. This result also agrees with our observations in a InGaAs-AlInAs MQW. In addition, Kwok *et al.* observed that the excited, parity forbidden transition $H1$-$E2$ shows a strong in-plane polarization. Their polarization data are shown in Fig. 4, together with our calculation. It appears that the agreement is reasonably good, if one accounts for the significant field inhomogeneity due to large carrier injection in this experiment. For this sample, Zhu and Chang [1] calculate a polarization rate of 0.5% at the onset of the $H1$-$H2$ transition for $F = 36$ kV/cm, to be compared with the $H_{\mathrm{BF}}$ result of 6.6%. Hence, the $H$-$L$ mixing at $\mathbf{k}_t = \mathbf{0}$ seems to also play the dominant role in the case of biased CA-QW's.

In conclusion, we have found that InGaAs-InP NCA-QWs show a giant optical anisotropy which can be tuned by an applied electric field. This original observation is very well described by the recent $H_{\mathrm{BF}}$ theory, in which the origin of these effects is a $\mathbf{k}_t = \mathbf{0}$ coupling of the heavy- and light-holes not taken into account by previous theories. Even in the case of CA-QWs, the $H_{\mathrm{BF}}$ perturbation terms are much larger than the bulk inversion asymmetry terms considered previously.

We thank Professor E. Ivchenko, Professor J. Khurgin, Professor D. Bertho, and Professor C. Jouanin, as well as our colleagues G. Bastard, R. Ferreira, L. Vervoort, and M. Voos for many passionate discussions of these results.

[1] B-F Zhu and Y. C. Chang, Phys. Rev. B **50**, 11 932 (1994).
[2] U. Rössler, Solid State Commun. **49**, 943 (1984); R. Winkler and U. Rössler, Phys. Rev. B **48**, 8918 (1993).
[3] J. N. Schulman and Y. C. Chang, Phys. Rev. B **31**, 2056 (1985); **31**, 2069 (1985).
[4] B. Jusserand, D. Richards, G. Allan, C. Priester, and B. Etienne, Phys. Rev. B **51**, 4707 (1995).
[5] O. Krebs, W. Seidel, J. P. André, D. Bertho, C. Jouanin, and P. Voisin, Semicond. Sci. Technol. **12**, 938 (1997).
[6] These anisotropy effects have been observed in many (InGa)As-InP and InP-(AlIn)As MQWs, as well as in InAs-GaSb heterostructures.
[7] S. H. Kwok, H. T. Grahn, K. Ploog, and R. Merlin, Phys. Rev. Lett. **69**, 973 (1992).
[8] O. Krebs and P. Voisin, Phys. Rev. Lett. **77**, 1829 (1996).
[9] G. E. Pikus and A. N. Titkov, in *Optical Orientation*, edited by F. Meier and B. P. Zakharchenya (Elsevier, New York, 1984).
[10] E. Ivchenko, A. Kaminski, and U. Rössler, Phys. Rev. B **54**, 5852 (1996); E. Ivchenko and A. Toropov (private communication).
[11] The nominal value $F = (V + V_0)/L_I$ is used to fit the whole set of data ($V$ is the bias, $eV_0$ the QW band gap, and $L_I$ the width of the intrinsic region).
[12] V. S. Bagaev, Y. N. Berozashvili, and L. V. Keldysh, JETP Lett. **4**, 246 (1966).
[13] A. G. Aronov and G. E. Pikus, Sov. Phys. Solid State **10**, 648 (1968).
[14] J. B. Khurgin and P. Voisin, Semicond. Sci. Technol. **12**, 1378 (1997).
[15] G. Bastard, J. A. Brum, and R. Ferreira, Solid State Phys. **44**, 229 (1991).
[16] J. A. Brum and G. Bastard, J. Phys. C **18**, L789 (1985).